

High-Strength Concrete at High Temperature – An Overview

Long T. Phan

ABSTRACT

This paper presents results of NIST's experimental program on the effects of elevated temperature exposure on the mechanical properties and potential for explosive spalling of high strength concrete (HSC). Mechanical properties of HSC were measured by heating 100 x 200 mm cylinders at 5 °C/min to temperatures of up to 600 °C, and heat-induced pore pressure buildup was measured by heating 100 x 200 x 200 mm blocks to the same temperature level at the same heating rate. The results of NIST mechanical property measurement are compared with results obtained in other studies as well as with existing code provisions to evaluate their applicability to HSC. The paper also presents results of measurement that indicate the efficacy of polypropylene fibers for mitigation of explosive spalling.

1 Introduction

Degradation of mechanical properties of concrete due to short-term exposure to elevated temperature has been studied as early as the 1950s. Among the early studies were those of Abrams [1], Malhotra [12], and Schneider [16,17]. Results of these studies constituted the technical basis for the provisions and recommendations for determining concrete strength at elevated temperature in many existing codes. While these studies provided valuable information on concrete strength as a function of temperatures, almost all used specimens made with normal strength concrete (NSC, $f_{23\text{C}} \leq 40$ MPa). Thus, in light of the results of recent studies, which have shown that high-strength concrete (HSC) behavior at elevated temperature may be significantly different from that of NSC [14,15,18-20], question may be raised as to whether existing design rules and recommendations are applicable to HSC.

The behavioral differences between HSC and NSC are found in two main areas: (1) the relative strength loss in the intermediate temperature range (100 °C to 400 °C) and (2) the occurrence of explosive spalling in HSC specimens at similar intermediate temperatures.

In terms of strength loss, studies [14,15,18,19] have shown that, for intermediate temperatures between 100 °C and 400 °C, the compressive strength of HSC could be reduced by close to 40 % of the room-temperature strength – a reduction of approximately 20 to 30 percentage points more than in NSC exposed to the same temperatures.

In terms of explosive spalling, which refers to a sudden and violent breaking away of a surface layer of heated concrete, it has been observed in laboratory tests that HSC has a significantly higher potential for explosive spalling than NSC, even at heating rates less than 5 °C/min which is lower than that would occur during real fires [4,7-10,15-18]. The phenomenon,

however, has been observed inconsistently, and there is not a complete understanding of the factors that control explosive spalling in HSC. The general feeling is that its occurrence is related to the inability of HSC, due its low permeability, to mitigate the buildup of internal pressure as free water and chemically-combined water are vaporized with increasing concrete temperature. The tendency for explosive spalling of HSC means that HSC structural elements may be more susceptible than NSC to losing the concrete cover that provides thermal protection for the steel reinforcement. None of the current codes addresses the tendency for explosive spalling of HSC.

Given the many benefits of HSC and its increased use in structural applications, it is essential that the fundamental behavior of HSC at elevated temperatures be understood to ensure that structural fire design involving HSC will be safe. This paper presents available test data on effects of elevated temperature exposure on HSC, including strength and pore pressure data recently obtained in the NIST experimental program. The paper compares the compiled test data with existing design rules to assess their applicability to HSC.

2 Test Programs and Results

2.1 NIST Test Programs

The experimental phase of the NIST study includes two series of experiments. One measured mechanical properties of HSC (strength, modulus of elasticity) at elevated temperature using 100 x 200 mm cylinders. The other measured internal pore pressure buildup in 100 x 200 x 200 mm concrete blocks, made with and without polypropylene fibers. The program to measure mechanical properties comprises of three series of tests on cylinders, corresponding to three steady-state temperature conditions, or three test methods (namely *stressed*, *unstressed*, and *unstressed residual property* test methods). The *stressed* and *unstressed* test methods were designed to provide measurements of property data *at elevated temperatures* and required simultaneous application of loading and heating. The *unstressed residual property* test method was designed to provide property data of concrete *at room temperature* after heating and cooling. In the *stressed* test, specimens were restrained by a preload equal to 40 percent of their room-temperature compressive strength ($0.4f_{230C}$) prior to and throughout the heating process. In the *unstressed* and *unstressed residual property* tests, the specimens were heated without restraint. Both *stressed* and *unstressed* specimens were loaded to failure at elevated temperature under uniaxial compression, when the steady-state temperature is reached within the specimen. This typically requires a 5h: 15min \pm 15min of heating at 5 °C/min and holding at a target temperature (up to 600 °C).

Mechanical property specimens were made from three HSC mixtures (named mixture I to III) and one NSC mixture (named mixture IV), using ASTM type I portland cement, crushed limestone and natural river sand. Table 1 lists information on the mixture proportion and properties of fresh and hardened concrete used in the NIST test program.

All mechanical property test specimens were cured under water at room temperature until test time. Before testing, the specimens were removed from the curing tank and the ends were ground to ASTM C 469 [3] requirements for perpendicularity and planeness. Fig. 1 shows the setup used for the stressed and unstressed tests. The specimen is placed at the center of the electric split-tube furnace with openings at the top and bottom to allow the loading rams to transmit compressive load from the test machine. For the *unstressed residual property* tests, the cylinders were heated

separately and allowed to cool down to room temperature before loading to failure (24 hours of natural cooling after heating).

Table 1—Mixture proportions and properties of concrete

		Mixture I ($w/c = 0.22$)	Mixture II ($w/cm = 0.33$)	Mixture III ($w/cm = 0.33$)	Mixture IV ($w/cm = 0.57$)
Materials	Cement (kg/m^3)	596	596	662	376
	Water (kg/m^3)	133	199	194	213
	Coarse aggregate* (kg/m^3)	846	846	846	854
	Fine aggregate* (kg/m^3)	734	734	734	868
	Silica fume	66	66	0	0
	HRWRA*** (mL/m^3)	400	354	154	0
Properties	Fresh concrete				
	Slump (mm)	240	230	35	76
	Air content (%)	3.2	2.8	2.0	2.5
	Hardened concrete				
	Initial moisture content (%)	5.0	6.1	6.3	7.3
	Compressive strength (MPa)				
	28-day	75.3	66.0	53.2	40.6
	58-day	86.7	79.5	58.9	41.9
	400-day	98.2	81.2	72.3	46.9
	Dynamic Modulus** (GPa)				
58-day	34.3	37.2	36.6	34.4	
400-day	47.2	43.7	44.1	36.7	

* Saturated surface-dry condition

** From longitudinal resonant frequency according to ASTM C 215 [2]

***High-Range Water Reducing Admixture

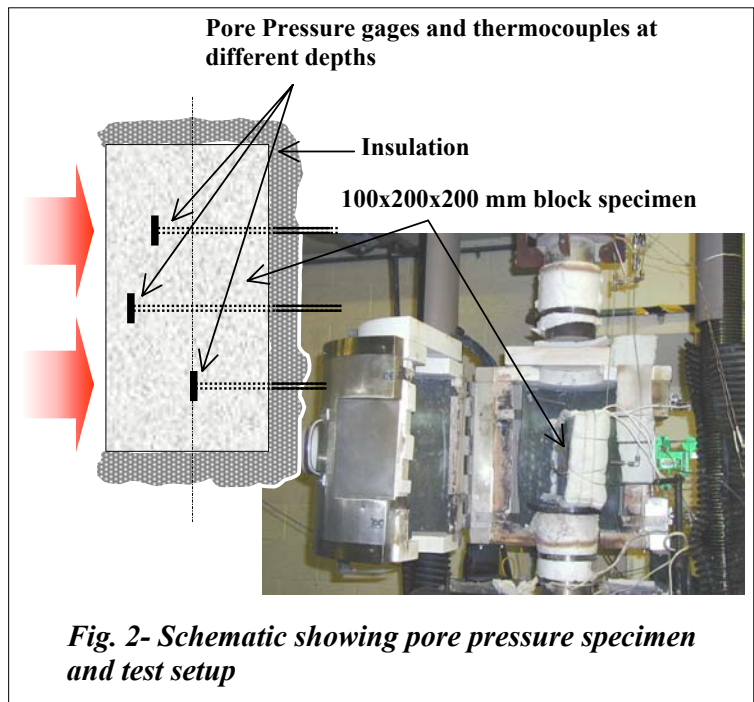
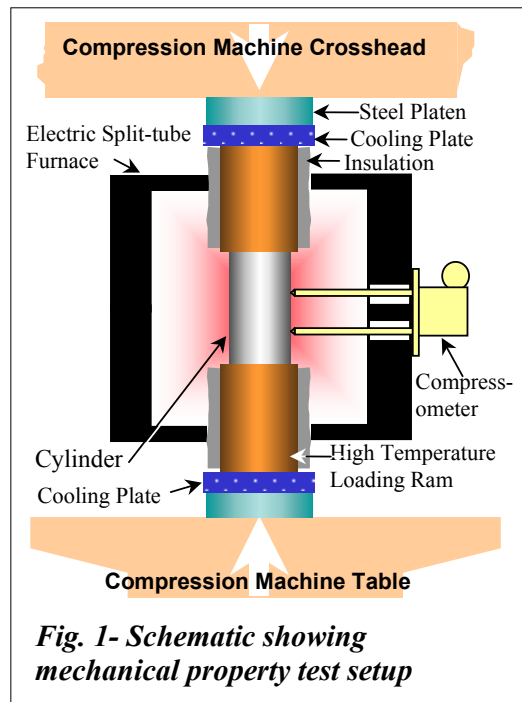
Pore pressure specimens (100x200x200 mm blocks) were made from HSC mixture I and NSC mixture IV. This test series was designed to study the effects of w/cm (0.22 and 0.57), initial moisture contents (caused by two different curing conditions: submerged and air-dried), dosages of poly propylene (PP) fibers (0, 1.5 kg/m^3 , and 3.0 kg/m^3), and heating rates (5 °C/min and 25 °C/min) on pore pressure development and potential for explosive spalling in HSC. The specimens were insulated on all sides, except the face, to simulate the one-dimensional heat flow condition that exists a concrete wall exposed to fire. All pore pressure specimens were instrumented with pressure gages and thermocouples at different depths (13 mm, 25 mm, 50 mm, and 75 mm from the heated face of the specimen) to measure pore pressure and temperature developments in the specimen. Figure 2 shows a pore pressure specimen inside the furnace.

2.2 Test Results

2.2.1 Heating Characteristics

Figure 3 (a) shows the temperature development in the furnace and a mixture I cylinder when exposed to target furnace temperature of 500 °C. The heating rate of the air in the furnace is 5

$^{\circ}\text{C}/\text{min}$ or $300\text{ }^{\circ}\text{C}/\text{h}$. It is noted that the concrete temperature lags the air temperature of the furnace. Figure 3 (b) shows the temperature difference between the surface and center of the cylinder, and the rates of temperature rise on the surface and at the center of the cylinder.



As shown in these figures, the temperature distribution inside the specimen has a complex history compared with the furnace air temperature. Figure 3(b) shows that there are “perturbations” in the rates of temperature rise that occur at different times during heating. In general, three types of perturbations were observed with increasing temperature [15]:

- a sudden decrease in the rate of temperature rise at the center;
- an increase in the rate of temperature rise on the surface and beginning of a simultaneous decrease in the temperature rise at the center; and
- an increase in the rate of temperature rise at the center.

Examples of these perturbations are marked in Fig. 3(a) and (b) by vertical dashed lines. It is believed that these perturbations are related to different stages of the moisture transformation and transport process (vaporization and movement of free and chemically bound water) that occur in the specimen during heating. The first two perturbations in the rates of temperature rise at the center and the surface of the specimen coincided with concrete temperatures of about $100\text{ }^{\circ}\text{C}$ and $180\text{ }^{\circ}\text{C}$ (see Fig. 3(a)). At slightly above $100\text{ }^{\circ}\text{C}$, free water in the concrete begins to evaporate rapidly. A moisture front is driven by the heat toward the center of the specimen, causing a decrease in the rate of temperature rise at the specimen center and thus an increase in the temperature difference between the cylinder’s surface and center. When the center reaches about $180\text{ }^{\circ}\text{C}$, a significant amount chemically bound water is released. This caused a similar decrease in the rate of temperature rise at center. In addition, the rate of temperature rise on the surface increases, presumably due to a reduction in the evaporative cooling effect, as marked by the second vertical dashed line in Fig. 3 (a) and (b).

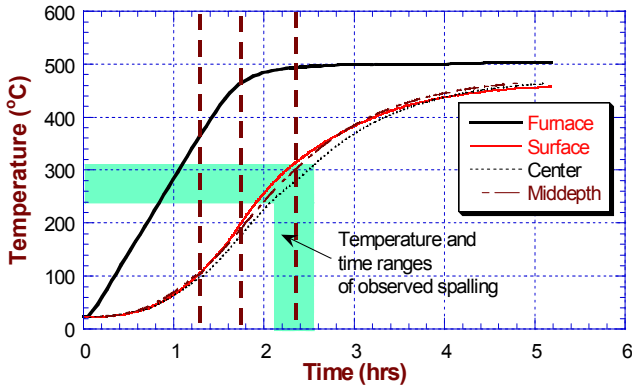


Fig. 3(a)–Temperature development in Mixture I cylinder

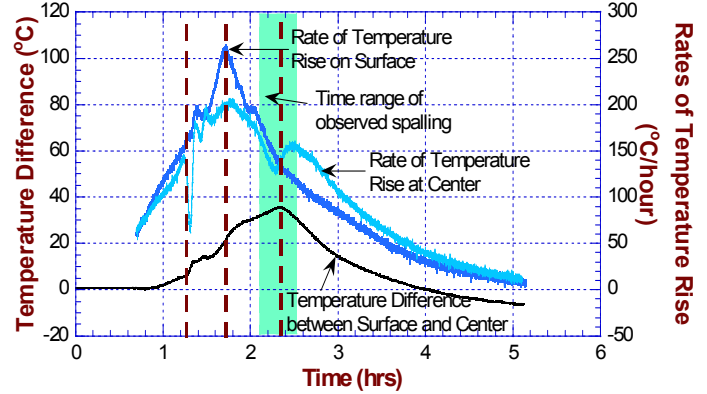


Fig. 3(b)–Temperature difference between surface and center of Mixture I cylinder

The temperature difference between the surface and center reaches a maximum of 36 °C at a corresponding center temperature of 270 °C. This coincides the third major perturbation in the rates of temperature rise in the cylinder. In this case there is a rapid increase in the rate of temperature rise at center (third vertical dashed line). After this point, the rate of temperature rise on the concrete surface is lower than that of the center, causing the temperature difference to decrease as shown in Fig. 3(b).

Similar perturbations in internal concrete temperature developments also occurred in the pore pressure block specimens, even though the heat flow in the block specimen is one-dimensional. Figure 4 shows the rates of temperature rise at points 25 mm and 50 mm deep from the heated surface of a mixture I specimen which suffered explosive spalling. Again, the vertical dashed lines mark the major perturbations in the rates of temperature rise in this specimen. Similar to the cylinder specimens, the three major perturbations in the block specimens also occurred at temperatures slightly above 100 °C, about 180 °C, and about 240 °C (at which temperature explosive spalling occurred in this specimen). These consistent heating characteristics, characterized by sudden changes in rates of temperature rise inside the concrete while the ambient temperature was rising at a constant rate, reveal a complex process of heat-induced moisture transformation and transport of free and chemically combined water that are unique to HSC. It is believed that this moisture transformation and subsequent transport of water and vapor contributed significantly to the buildup of pore pressure that causes explosive spalling in HSC.

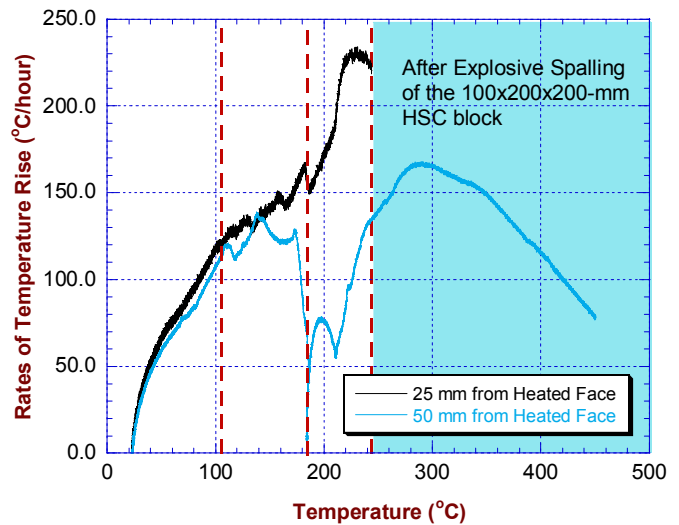


Fig. 4–Rates of temperature rise and perturbations in pore pressure specimen

2.2.2 Spalling Characteristics and Pore Pressure

Explosive spalling is characterized by the sudden fragmentation of the specimens during heating. This is accompanied by a loud bang and the instantaneous release of a large amount of energy that propels the fragments at high velocity in all directions. Table 2 shows the test matrix and the incidences of explosive spalling in the mechanical property test series. Each circle in this table represents a cylinder test and an open circle represents a cylinder that exploded while being heated to the target temperature. Examination of exploded cylinders showed that typically there was a large intact core, measured approximately 70 x 120 mm, which was surrounded by an approximately 20 mm-thick outer concrete shell (see Fig. 5). It appears that explosive spalling of the cylinders occurs by separation of the 20 mm thick shell from the core. This is consistent with the notion that explosive failure results from the build up of internal vapor pressure.

A study of Table 2 shows the following tendencies for spalling in cylinder specimens:

- For the *stressed* tests, all cylinders of mixtures II and III exploded while being heated to 600 °C, while cylinders of mixtures I and IV did not experience any explosive spalling.
- For the *unstressed* tests, all cylinders of mixture I and one of four cylinders of mixture II exploded while being heated to 450 °C, and all cylinders of mixtures II and III exploded while being heated to 600 °C (mixture I specimens were not heated to 600 °C due to the consistent failure while being heated to 450 °C).
- For the *unstressed residual property* test, one cylinder from each group of mixtures I and II exploded while being heated to 300 °C, and all mixture I cylinders exploded while being heated to 450 °C.

Table 2–Test Matrix

Test Methods and Target Temperatures		w/cm =0.22	w/cm =0.33		w/cm =0.57
		Mixture I (98 MPa)	Mixture II (88 MPa)	Mixture III (75 MPa)	Mixture IV (50 MPa)
		With Silica Fume		Without Silica Fume	
Stressed	25 °C	● ● ●	● ● ●	● ● ●	● ● ●
	100 °C	● ● ● ● ●	● ● ●	● ● ●	● ● ●
	200 °C	● ● ●	● ● ●	● ● ●	● ● ●
	300 °C	● ● ●	● ● ●	● ● ●	● ● ●
	450 °C	● ● ●	● ● ●	● ● ●	● ● ●
	600 °C	● ● ●	○ ○ ○	○ ○ ○	● ● ●
Unstressed	25 °C	● ● ●	● ● ●	● ● ●	● ● ●
	100 °C	● ● ●	● ● ●	● ● ●	● ● ●
	200 °C	● ● ●	● ● ●	● ● ●	● ● ●
	300 °C	● ● ●	● ● ●	● ● ●	● ● ●
	450 °C	○ ○ ○	● ● ● ○	● ● ●	● ● ●
	600 °C	Not Tested	○ ○ ○	○ ○ ○	● ● ●
Unstressed Residual Property	25 °C	● ● ●	● ● ●	● ● ●	● ● ●
	100 °C	● ● ●	● ● ●	● ● ●	● ● ●
	200 °C	● ● ●	● ● ●	● ● ●	● ● ●
	300 °C	● ● ● ○	● ● ● ●	● ● ●	● ● ●
	450 °C	○ ○ ○	● ● ●	● ● ●	● ● ●

● Test specimen that failed in uniaxial compression
○ Test specimen that failed by explosive spalling

At the time of this writing, the pore pressure test series has been completed. However, rigorous statistical analysis of test data to quantify the effects of the variables mentioned in section 2.1 is not yet completed. Thus, only qualitative results are shown (Figures 6 and 7) and discussed here.

Figure 6 shows pore pressure developments at points 25 mm and 50 mm deep (from the heated face) in a 100 x 200 x 200 mm specimen (HSC



Fig. 5 – Remnants of an exploded cylinder and rendering of fracture formation

mixture I ($w/cm=0.22$), no PP fiber, moist-cured, heated at $5\text{ }^{\circ}\text{C}/\text{min}$) that exploded. Typically, regardless whether explosive spalling occurred, maximum pore pressure is observed at point 25 mm deep. For this particular specimen, the maximum pore pressure in a specimen, reached before explosive spalling, was 2.1 MPa. Note that even after spalling, which delaminated and fragmented a surface layer with nominal thickness of about 25 mm, pore pressure continued to build at point 50 mm deep, which is inside the intact portion of the specimen.

Figure 7 shows pore pressure developments as a function of temperature at 25 mm deep in 5 different specimens. The descriptions of the specimens are summarized on the figure. Comparisons of pore pressure developments shown in this figure indicate the significant role of w/cm (implicitly permeability) and initial moisture content on pore pressure buildup and explosive spalling (pore pressure in both mixture IV specimens was able to attenuate gradually after reaching maximum of 1.3 MPa and 0.4 MPa, while mixture I specimen exploded at 2.1 MPa). The results shown in Figure 7 also show the effectiveness of PP fibers as a means to mitigate the buildup of pore pressure. Instead of reaching the critical explosive spalling pressure, the additions of $1.5\text{ kg}/\text{m}^3$ and $3.0\text{ kg}/\text{m}^3$ PP fibers in HSC mixture I resulted in reduced maximum pore pressure to levels comparable with those observed in NSC specimens.

The mean concrete temperatures (at 25 mm deep in the cylinder and blocks) when explosive spalling occurred was about $250\text{ }^{\circ}\text{C}$, with an approximate range of $\pm 50\text{ }^{\circ}\text{C}$ (see Figs. 3(a), 3(b) and 7). As can be seen in Fig. 3(b), the temperature range in which explosive spalling occurred coincides with the time of high thermal gradient between the surface and center. This suggests that, while internal pore pressure may be the primary cause for the explosive spalling of the specimens, the buildup of thermally induced strains might have a secondary role in this failure.

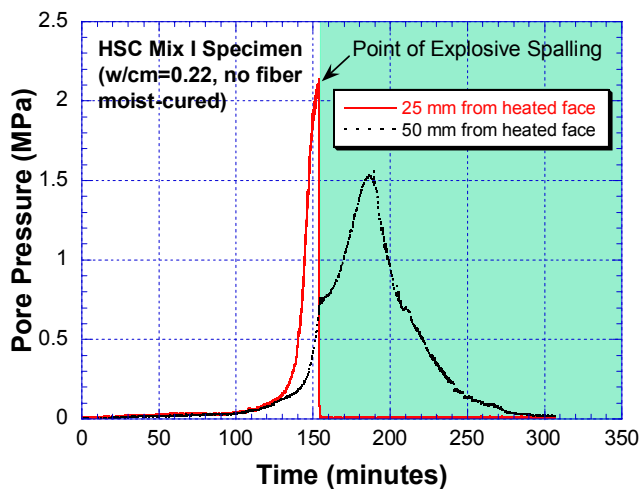


Fig. 6 – Pore pressure developments at different depths inside a block specimen

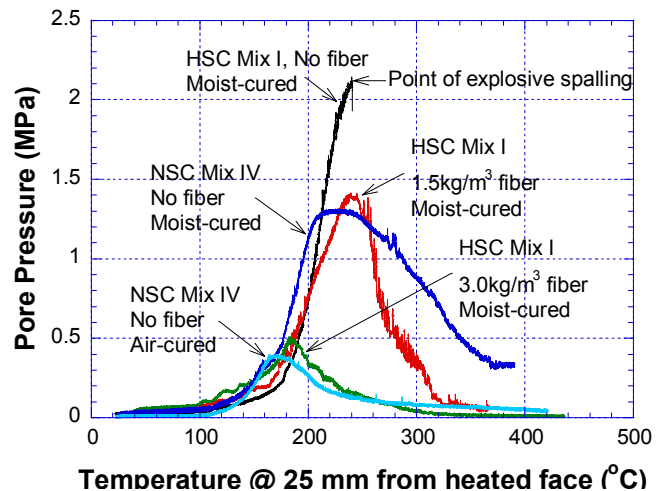


Fig. 7 – Pore pressure at 25 mm deep in different block specimens

2.2.3 HSC Mechanical Properties

Mechanical property data obtained from NIST and other studies are compiled and shown in Table 3. While it is recognized that differences in the heating conditions (i.e., exposure time, heating rate), type of aggregate, shape and size, specimen curing condition and so forth, used in different test programs could result in measurements that are not directly compatible, it is

necessary to compare the NIST results with those of others based only on the test methods since there are insufficient data to be normalized with respect to all the applicable variables.

Table 3 – Summary of information on elevated temperature tests of concrete by various studies

Test Methods and Programs		Specimen	$f_{23\text{ }^{\circ}\text{C}}$ (MPa)	w/cm	Silica Fume (% by mass)	Preload (% of $f_{23\text{ }^{\circ}\text{C}}$)	Heating Rate ($^{\circ}\text{C}/\text{min}$)
Stressed	NIST Mixture I	100 x 200	98	0.22	10	40	5
	NIST Mixture II	100 x 200	88	0.33	10	40	5
	NIST Mixture III	100 x 200	75	0.33	0	40	5
	NIST Mixture IV	100 x 200	50	0.57	0	40	5
	Castillo and Durani	51 x 102	89	0.33	0	40	7 to 8
	Khoury and Algar	60 x 180	85	0.32	0	20	2
	Abrams	75 x 150	45	unknown	0	40	unknown
Unstressed	NIST Mixture I	100 x 200	98	0.22	10	0	5
	NIST Mixture II	100 x 200	88	0.33	10	0	5
	NIST Mixture III	100 x 200	75	0.33	0	0	5
	NIST Mixture IV	100 x 200	50	0.57	0	0	5
	Castillo and Durani	51 x 102	63, 31	0.33, 0.68	0	0	7 to 8
	Hammer	100 x 310	68 to 118	0.27 to 0.50	5	0	2
	Diederichs et al.	100x100x100 and 80x300	33 to 114	0.26 to 0.45	10	0	2, 32
	Furumura et al.	150 x 300	55, 79	0.41, 0.32	0	0	1
	Khoury and Algar	60 x 180	85	0.32	0	0	2
	Abrams	75 x 150	23	unknown	0	0	unknown
Unstressed Residual Property	NIST Mixture I	100 x 200	98	0.22	10	0	5
	NIST Mixture II	100 x 200	88	0.33	10	0	5
	NIST Mixture III	100 x 200	75	0.33	0	0	5
	NIST Mixture IV	100 x 200	50	0.57	0	0	5
	Hertz	100 x 200 57 x 100 28 x 52	150		1, 5, 10, 15, 20	0	1
	Morita et al.	100 x 200	20 to 74		0	0	1
	Felicetti et al.	100 x 300	72, 95	0.43, 0.30	9.4, 6.7	0	0.2
	Khoury and Algar	60 x 180	85	0.32	0	0	2
	Abrams	75 x 150	23, 45	unknown	0	0	unknown

Stressed Test Data

Fig. 8 shows the relative strength – temperature relationships of HSC (solid lines) and NSC (dashed lines) obtained under the *stressed* test method. As is shown in this figure, there is only a limited amount of test data available for this test condition prior to the NIST test series. This is probably due to the difficulty in applying and maintaining the constant preload on the test specimen while it is being heated simultaneously. In Fig. 8, NIST data are shown in thick solid

lines with symbols. The symbols represent the mean measured strengths of at least three specimens at a particular temperature. The range of NIST test results was shaded for convenience.

The NIST test results showed that HSC sustained an average strength loss of about 25 % at 100 °C. This is consistent with data by Castillo and Durrani [4] at up to 200 °C and with data by Khoury and Algar [11] at 100 °C. Data for NSC by Abrams [1], however, indicated a slight strength gain for siliceous NSC and no effect on strength for calcareous NSC in this temperature range.

Strength data at 600 °C for NIST mixtures II and III are not available due to explosive spalling of the specimens while being heated to this temperature. Castillo and Durrani [4] reported explosive spalling in about one third of the specimens being heated to 700 °C while Khoury and Algar [11] did not mention explosive spalling. Detailed discussion concerning the effects of temperature, w/cm , preload level, and silica fume on concrete strength examined in the NIST study, as well as summaries of findings from other studies, may be found in [15,18].

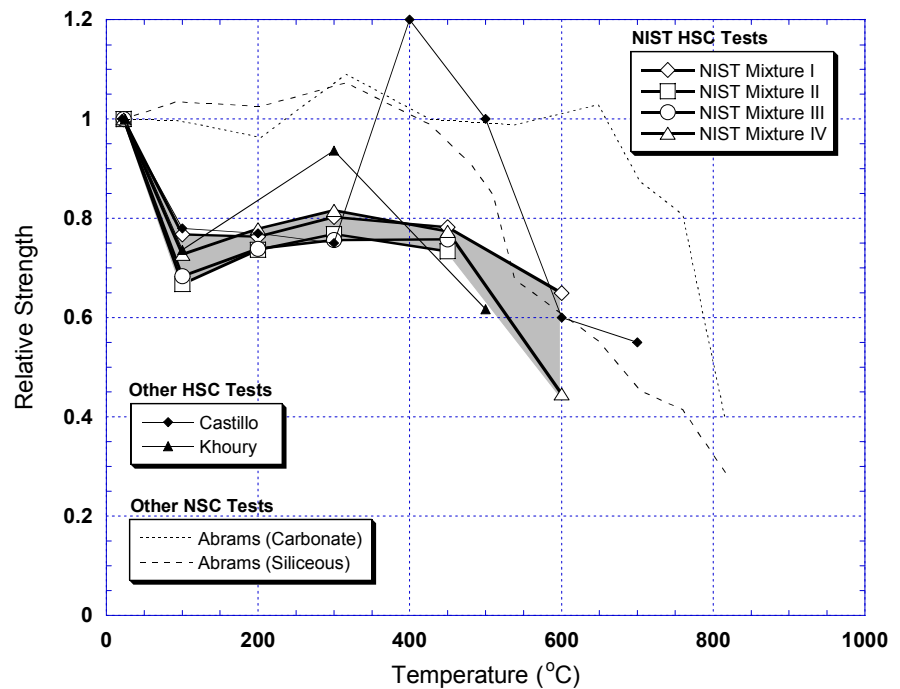


Fig. 8 — Stressed Test Results

Unstressed Test Data

More data are available for the *unstressed* tests than for the stressed tests, as shown in Table 3 and Fig. 9. The strength-temperature relationships observed in the NIST's *unstressed test* data are similar in trend with those of the NIST's *stressed test* data, except that the strength losses in the unstressed tests are slightly larger at each target temperature. The NIST strength-temperature relationships also followed the general trend of unstressed HSC tests reported by Hammer [8] and Diederichs et al. [9,10], which constituted the majority of the unstressed test data for HSC. In general, within the intermediate temperature range of 100 °C to 450 °C, most studies reported higher strength loss for HSC compared to NSC.

More incidences of explosive spalling were observed in the NIST study under this test condition. As a result, NIST mixture I has no strength data above 300 °C, and mixtures II and III have no strength data above 450 °C. Spalling did not occur in any of the mixture IV specimens.

Diederichs et al. [9,10], Hammer [8], and Furumura et al. [6] also reported explosive spalling failure of their unstressed HSC specimens, even though some of these studies used very low heating rates (1 °C/min for Furumura and 2 °C/min for Hammer). Study by Castillo and Durrani [4], however, indicated that explosive spalling occurred only in their stressed test specimens and none occurred under unstressed test condition.

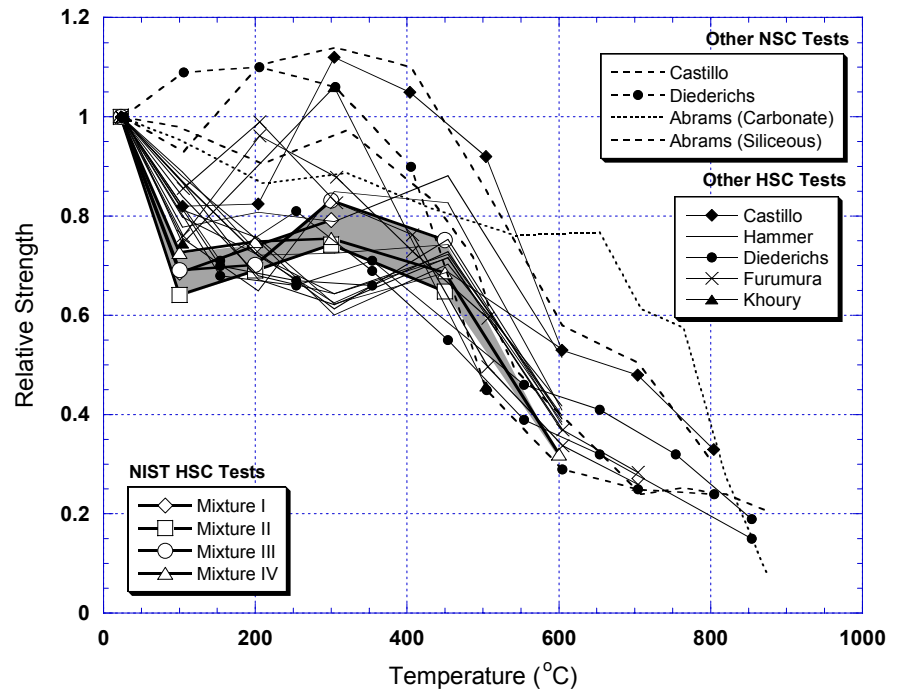


Fig. 9-Unstressed Test Results

Unstressed Residual Property Test Data

Fig. 10 shows the strength-temperature relationships for the *unstressed residual property* test. NIST test data showed a wider range of strength loss between the four mixtures under this test method than in the *stressed* or *unstressed* test methods. The NIST test results at under 200 °C also differed from data for both HSC and NSC in other studies. The largest difference is at 100 °C, at which the NIST results showed a strength loss ranging between 10 % to 30 % while data for HSC from other studies showed either a strength gain or loss of a little more than 5 %. At above 300 °C, the average difference in relative strengths between test programs appeared to be insignificant. The temperature rates of strength reduction between test programs are also similar.

Explosive spalling occurred in one (out of five) NIST mixture I and one (out of four) mixture II specimens while they were being heated to 300 °C. Explosive spalling also occurred in all mixture I specimens while

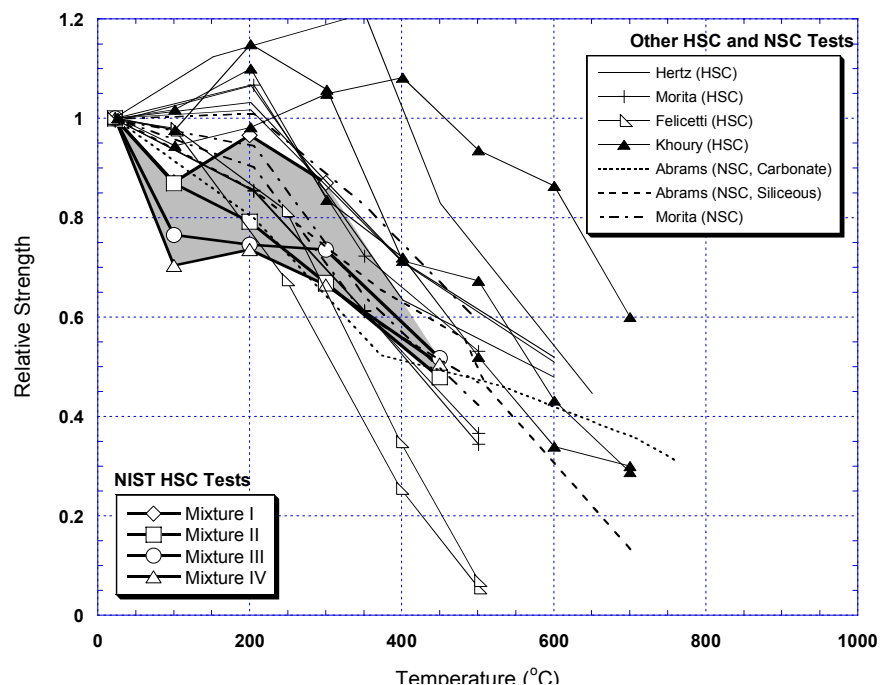


Fig. 10-Unstressed Residual Strength Test Results

they were being heated to 450 °C. Again, explosive spalling did not occur in any of the NIST mixture IV specimen. Of the referenced studies, only that of Hertz [7], which used ultra high strength concrete, reported explosive spalling in the unstressed residual property test.

3 Comparisons with Codes

The compiled test data are compared with the provisions for computing concrete strength at elevated temperature prescribed by existing codes. Among the codes which specify design rules for computing concrete strength at elevated temperature are the Comité Européen de Normalisation (CEN ENV [21], Eurocode 2 - *Part 1-2: Structural Fire Design* and Eurocode 4 - *Part 1-2 General Rules for Structural Fire Design*), the Comites Euro-International du Beton (CEB model code) Bulletin D'Information N° 208, 1991, *Fire Design of Concrete Structures* [22], and the National Building Code of Finland's RakMK B4 [23].

The CEN ENV and CEB make no distinction between HSC and NSC in their fire design provisions. Thus, their design rules are compared to both HSC and NSC data. Furthermore, while the CEN ENV and the CEB did not explicitly prescribe whether their design rules were specified for concrete in service (i.e. concrete under service load), it is assumed that this is the case since both codes are for the design of structural concrete. Thus, the design rules prescribed by CEN ENV and CEB will be compared with the data of the stressed tests. It should be noted that, at the time of this writing, it is believed that the provisions for concrete strength at elevated temperature of the CEN ENV are being revised by CEN Technical Committee 250. The revisions take into account the difference in concrete strength grades and also provide measures for mitigating explosive spalling problem in HSC (PP fibers).

Finland's *RakMK B4* prescribes different design rules for HSC and NSC. HSC is concrete with designated strength grades of K70 to K100 (concretes with 70 MPa to 100 MPa compressive strength if 150 mm cubes are used, or 62 to 90 MPa if 150 x 300 mm cylinders are used). NSC is concrete with designated strength grades of K10 to K70 (concretes with 10 MPa to 70 MPa compressive strength if 150 mm cubes are used, or 7 MPa to 62 MPa if 150 x 300 mm cylinders are used). The *RakMK B4* also prescribes different design rules for concrete in service (stressed, $0.3f_{23,0C}$) and for concrete which is not (unstressed). Thus, the applicability of *RakMK B4* will be assessed by comparing with both the *stressed* and *unstressed* test data.

Also, comparisons with *unstressed residual* strength tests will not be made here since the code provisions were prescribed for concrete strength "at" elevated temperature, and not for concrete strength at room temperature after exposure to elevated temperature.

3.1 Comparisons of *Stressed* Test Data with Codes

Figure 11 shows the strength-temperature relationships obtained under the stressed test method for four HSC mixtures in this test program and in studies by Castillo and Durrani [4], Khoury and Algar [11] and Abrams [1]. The design rules for calculating concrete compressive strength at elevated temperatures, prescribed by the Eurocodes for calcareous aggregate concrete and siliceous aggregate concretes, and by the CEB, are superposed over the measured compressive strength-temperature relationships to provide an assessment of their applicability to HSC. It should be noted that since carbonate crushed limestones were used as coarse aggregate

in the four concrete mixtures tested in this test program, the Eurocode’s prescription for calcareous aggregate concrete is to be used in the comparison with the NIST test results.

As shown in Figure 11, the Eurocode’s strength-temperature relationship for calcareous aggregate concrete is unconservative when used for estimating compressive strength of HSC at temperatures less than 450 °C. The largest overestimation by the Eurocode was by about 20 percent. Above 450 °C, the strength loss prescribed by the Eurocode becomes more consistent with both HSC and NSC data. The unconservative estimation of HSC’s compressive strength by the Eurocode at temperatures less than 450 °C is more significant when explosive spalling, which is not addressed by the current Eurocode but observed in this test program in the intermediate temperature range is considered.

Similarly, the provisions of CEB were also based on NSC test data and are found to be unconservative when used for estimating HSC compressive strength at temperatures less than 350 °C. The largest overestimation by the CEB model code is by about 25 % at temperatures less than 200 °C. The

CEB’s rate of strength loss at temperature above 350 °C is consistent with data for both HSC and NSC. Also similar to the Eurocode, the unconservative estimation of HSC compressive strength by the CEB model code at temperatures less than 350 °C is more significant since the CEB does not address the explosive spalling problem observed for HSC in this temperature range.

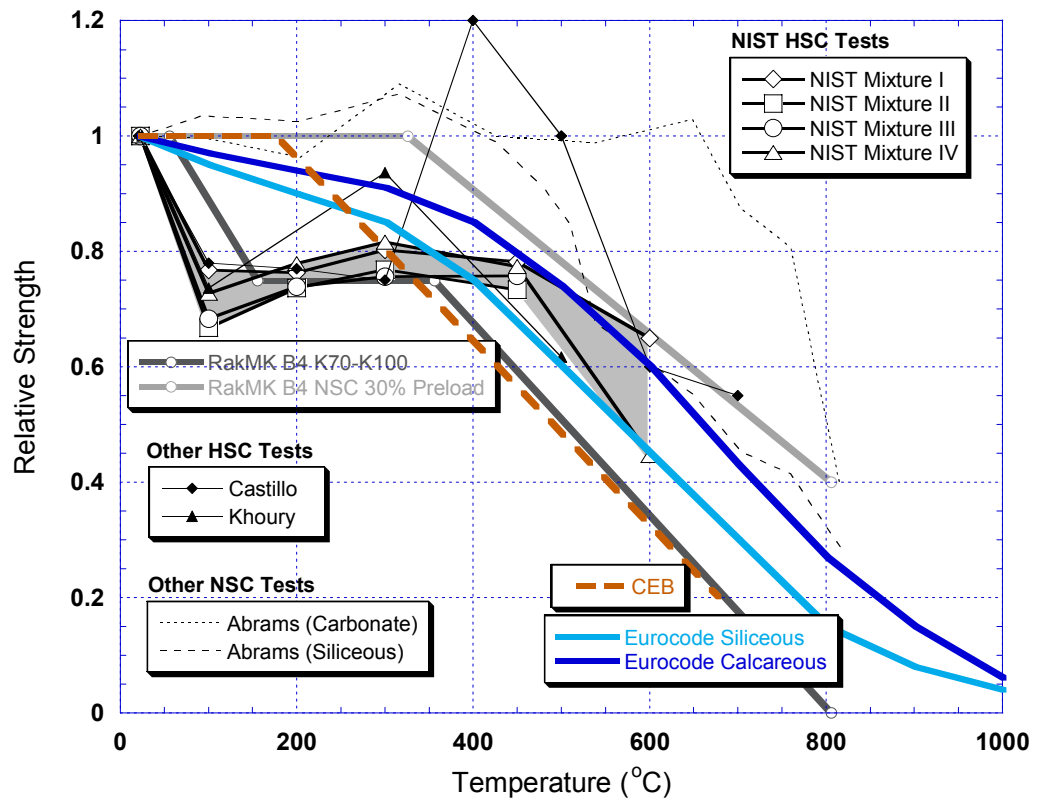


Fig. 11–Comparison of stressed test data with codes

The RakMK B4’s provision for NSC’s strength at elevated temperature with 30 percent preload is shown as the thick gray line with open circle symbol in Figure 11. This provision for NSC is also applicable to light weight aggregate concrete with preload of up to 30 percent the room temperature compressive strength of concrete. The RakMK B4’s provision for HSC’s strength at elevated temperature with 0 to 30 percent preload is shown as the thick dark line with open circles in Figure 11. The RakMK B4 provision for in-service concrete (stressed) of K10 to K70 strength grades (NSC) is consistent with the stressed test data for NSC up to 800 °C. The RakMK B4 provision for concrete with K70 to K100 strength grades appears to be slightly

unconservative at temperatures below 150 °C. However, this is to a much lesser degree compared with the Eurocode CEN ENV and the CEB. In the intermediate temperature range (150 °C and 350 °C), the RakMK B4 provision for in-service HSC is consistent with the NIST test data. From 350 °C to 800 °C, the RakMK B4 provision appears to be conservative compared with all test data, and is similar to the strength estimation prescribed by the CEB model code.

3.2 Comparisons of *unstressed* test data with codes

The RakMK B4’s prescription for strength-temperature relationship for HSC under *unstressed* test is similar to that of the stressed test. This prescribed relationship is superposed over the *unstressed* test data on Figure 12. The prescription for NSC under unstressed test differs from the prescription for NSC under stressed test shown previously in Figure 11. This is also superposed on Figure 12 (RakMK B4 NSC No Preload).

Similar to the *stressed* test, the RakMK B4’s strength provision for HSC appears to be slightly unconservative at temperatures below 150 °C with respect to the NIST’s test data. However, the RakMK B4’s prescription for HSC appears to be consistent with the average of all test measurements when results of other studies are combined with the NIST test results. Between 150 °C and 350 °C, the RakMK B4’s strength predictions are consistent with the NIST test data and the average of all existing unstressed test results for HSC. At temperatures above 350 °C, the RakMK B4 prescribes a period of progressive strength loss that is consistent with the strength losses observed in NIST and other studies. The RakMK B4’s strength prediction for unstressed NSC prescribes a range of no strength loss between room temperature and 220 °C. This is consistent with the average results of tests by Castillo and Durrani [4], Abrams [1], and Diederichs et al. [9,10]. Above 220 °C, RakMK B4 prescribes a strength loss period that has a similar rate of strength reduction as in the case for HSC. The prescribed strength loss is on the conservative side of the test data.

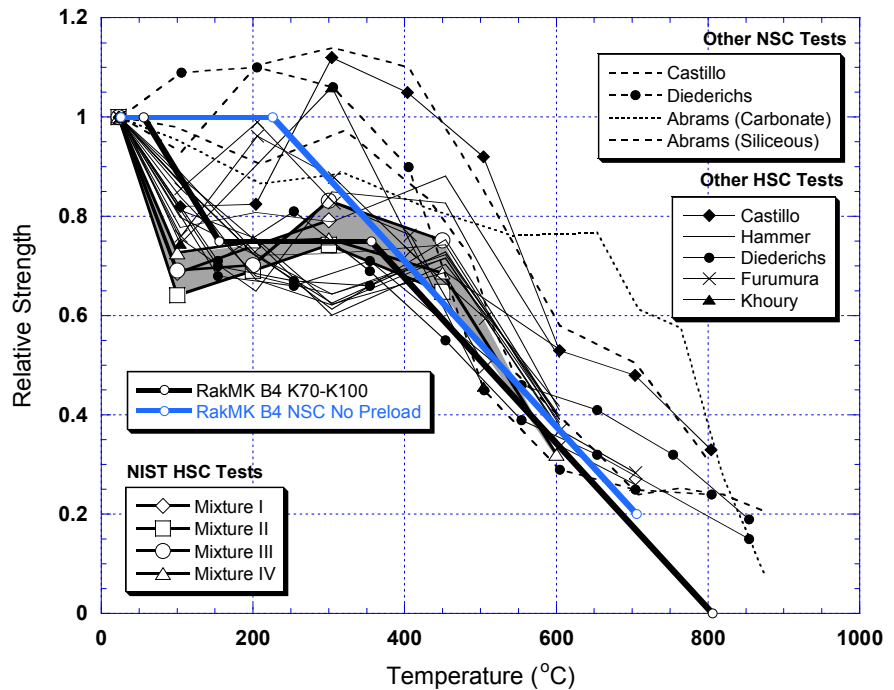


Fig. 12–Comparison of Unstressed Test Results with Code

4 Conclusions

- Internal concrete temperature histories provided insights into the moisture transport process in HSC. They revealed consistent perturbations in the rates of temperature rise inside the specimens, which are related to the transformations and subsequent transport of free and

chemically combined water. This shows that accurate modeling of temperature development in concrete needs to take into account the heat-induced moisture transformation and transport.

- The concrete temperatures (at 25 mm deep) when explosive spalling occurred ranged from 200 °C to 325 °C. Explosive spalling appeared to coincide with high pore pressure buildup and high thermal gradient. This suggests that, while internal pressure may be the primary cause of explosive spalling, thermal stresses may have a secondary role in this failure.
- HSC that carried a preload equal to 40 % of the room-temperature strength (stressed test condition) sustained, on average, the smallest strength loss due to temperatures up to 600 °C.
- The strength losses measured by the three test methods differed with exposure temperature. For temperatures of 100 °C and 200 °C, *residual property* test resulted in the lowest relative strength loss (on the order of 20 %, compared with 25 % to 30 % for the stressed and unstressed conditions). For exposure to 450 °C, the relative strength loss was highest for the *residual property* test (on the order of 50 %, compared with 25 % to 30 % for the other methods). These results indicate that there is a complex relationship between the strength measured at elevated temperature and the residual strength measured at room temperature.
- HSC mixture with the lowest w/cm of 0.22 sustained, on average, the lowest loss in relative strength (about 20 % compared with about 30 % for $w/cm = 0.33$ and 0.57).
- The effect of w/cm on relative strength was not the same for each test condition. For the unstressed test condition, there was no statistically significant difference in relative strength loss due to w/cm . For the stressed and residual property test conditions, however, mixture I with $w/cm = 0.22$ experienced less loss in relative strength.
- Overall, the presence of silica fume had no statistically significant effect on the relative strength loss. There was, however, some dependence on test condition. For the unstressed test condition, mixtures III and IV without silica fume had less strength loss than mixtures I and II with silica fume. For the other test conditions, the presence of silica fume had no overall statistically significant effects.
- With respect to explosive spalling, it was observed that the tendency was reduced in the stressed tests in which a compressive stress equal to 40 % of the room temperature strength was maintained during heating. As expected, there was an increase in spalling tendency as the w/cm decreased. This is consistent with the notion that the tendency for explosive spalling is related to the resistance to water vapor transport during heating. There was no clear evidence that the presence of silica fume by itself affects the tendency for explosive spalling.
- Significant reduction in pore pressure in HSC can be achieved with additions of PP fibers in the mixture. Reduction in pore pressure appeared to increase with increasing dosages (up to 3.0 kg/m³). Addition of 1.5 kg/m³ appeared sufficient to avoid explosive spalling.
- The Eurocode [21] and CEB [22] strength-temperature relationships are unconservative for estimating strength of HSC at high temperature. The largest overestimation is by about 20 % (Eurocode) and 25 % (CEB) at temperatures less than 450 °C. These overestimations are even more significant when explosive spalling is considered.
- Finland's RakMK B4 [23], which considers the differences in concrete strength grades and preload levels, is only slightly unconservative when compared with the test results. The slightly unconservative estimates by the RakMK B4 is at temperatures below 150 °C. However, this is to a much lesser degree compared to the levels of unconservative estimation by the Eurocode and the CEB. The RakMK B4's strength prediction for NSC at elevated temperatures is found to be consistent with NSC test results.

5 References

- [1] Abrams, M.S., “Compressive Strength of Concrete at Temperatures to 1600 °F,” American Concrete Institute (ACI) SP 25, Temperature and Concrete, Detroit, Michigan, 1971.
- [2] ASTM C 215-91, “Standard Test Method for Fundamental Transverse, Longitudinal, and Torsional Frequencies of Concrete Specimens”
- [3] ASTM C 469-94, “Standard Test Method for Static Modulus of Elasticity and Poisson’s Ratio of Concrete in Compression”
- [4] Castillo, C. and Durrani, A. J., “Effect of transient high temperature on high-strength concrete,” *ACI Materials Journal*, v. 87, no. 1, Jan-Feb 1990, p 47-53.
- [5] Felicetti, R.; Gambarova, P.G.; Rosati, G.P.; Corsi, F.; Giannuzzi, G.; “Residual Mechanical Properties of HSC Subjected to High-Temperature Cycles,” *Proceedings, 4th International Symposium on Utilization of High-Strength/High-Performance Concrete*, Paris, France, 1996, pp. 579-588.
- [6] Furumura, F.; Abe, T.; Shinohara, Y.; “Mechanical Properties of High Strength Concrete at High Temperatures,” *Proceedings, Fourth Weimar Workshop on High strength Concrete: Material Properties and Design*. Hochschule für Architektur und Bauwesen (HAB), Weimar, Germany, October 4th and 5th, 1995, pp. 237 - 254.
- [7] Hertz K., “Heat Induced Explosion of Dense Concretes,” Institute of Building Design, Report No. 166, Technical University of Denmark, 1984.
- [8] Hammer, T.A.; “HIGH-STRENGTH CONCRETE PHASE 3, Compressive Strength and E-modulus at Elevated Temperatures,” SP6 Fire Resistance, Report 6.1, SINTEF Structures and Concrete, STF70 A95023, February, 1995.
- [9] Diederichs, U., Jumppanen, U.M., Penttala, V., ‘Behavior of high strength concrete at high temperatures’, *Report #92*, Helsinki University of Technology (1989).
- [10] Diederichs, U., Jumppanen, U-M., Schneider, U., ‘High temperature properties and spalling behavior of high strength concrete’, *Proceedings, Fourth Weimar Workshop on High Performance Concrete: Material Properties and Design*, Hochschule für Architektur und Bauwesen. Weimar, Germany, October 4-5, 1995, PP. 219-236.
- [11] Khoury, G.; and Algar, S., ‘Mechanical behavior of HPC and UHPC concretes at high temperatures in compression and tension’, paper presented at ACI International Conference on State-of-the-Art in High Performance Concrete, Illinois, March 1999.
- [12] Malhotra, H.L., ‘The effect of temperature on the compressive strength of concrete’, *Magazine of Concrete Research*, v.8 (22) (London, 1956), 85-94.
- [13] Morita, T., Saito, H., and Kumagai, H., ‘Residual mechanical properties of HSC members exposed to high temperature-Part 1: Test on material properties’, *Summaries of Annual Meeting*, Architectural Institute of Japan, Niigata, August, 1992.
- [14] Phan, L.T.; and Carino, N.J., ‘Review of mechanical properties of HSC at elevated temperature’, *Journal of Materials in Civil Engineering*, American Society of Civil Engineers, v. 10 (1) (February, 1998) 58-64.
- [15] Phan, L.T.; Carino, N.J., ‘Mechanical Properties of High Strength Concrete at Elevated Temperatures’, NISTIR 6726, Building and Fire Research Laboratory, National Institute of Standards and Technology, Gaithersburg, Maryland, March 2001.
- [16] Schneider U., ‘Concrete at high temperatures-A general review’, *Fire Safety Journal*, The Netherlands (1988) 55-68.
- [17] Schneider, U., ‘Properties of materials at high temperatures-Concrete’, *RILEM-Committee 44-PHT*, Department of Civil Engineering, University of Kassel, Kassel, June, 1985.
- [18] Phan, L.T.; Carino, N.J., ‘Effects of test conditions and mixture proportions on behavior of high-strength concrete exposed to high temperatures’, *ACI Materials Journal*, American Concrete Institute, v. 99 (1) (January-February, 2002) 54-66.
- [19] Phan, L.T.; Lawson, J.R.; Davis, F.R., ‘Effects of elevated temperature exposure on heating characteristics, spalling, and residual properties of high performance concrete’, *RILEM Materials and Structures Journal*, v. 34 (236) (March 2001) 83-91.
- [20] George C. Hoff, “Fire Resistance of High-Strength Concretes for Offshore Concrete Platforms,” *Proceedings, Third CANMET/ACI International Conference*, ACI SP-163, V.M. Malhotra, Editor, pp. 53-87.
- [21] Comité Européen de Normalisation, ‘prENV 1992-1-2: Eurocode 2: Design of Concrete Structures. Part 1 -2: Structural Fire Design’, *CEN/TC 250/SC 2* (1993).
- [22] Comites Euro-International Du Béton, ‘Fire Design of Concrete Structures-in accordance with CEB/FIP Model Code 90’, *CEB Bulletin D’Information No. 208* (Switzerland, 1991).
- [23] Concrete Association of Finland, ‘High Strength Concrete Supplementary Rules and Fire Design’, *RakMK B4* (1991).